QUANTIFYING SHALLOW DEPTH CONCRETE DELAMINATIONS USING IMPACT ECHO

by

MANTAKA MAHJABIN MOMO

Presented to the Faculty of the Graduate School of

The University of Texas at Arlington in Partial Fulfillment

of the Requirements

for the Degree of

MASTER OF SCIENCE IN CIVIL ENGINEERING

THE UNIVERSITY OF TEXAS AT ARLINGTON

August 2020

Acknowledgements

First of all, I would like to express my sincere gratitude to my advisor, Dr. Nur Yazdani, for his consistent guidance and continuous support throughout my research. I am thankful to him for giving me the opportunity to work under his supervision. I would also like to thank Dr. Laureano Hoyos and Dr. Mohsen Shahandashti for accepting to serve as my thesis committee member and provide me with their valuable suggestions.

My sincere appreciation goes to Dr. Eyosias Beneberu for helping me establish the basis of this research work and for providing me with his consistent review and encouragement. I am also thankful to my fellow lab members who helped and guided me during different stages of my research work.

I would like to convey my respect to my family members who have always encouraged and supported me to continue my study and research. Last but not the least, I would like to offer my heartiest gratitude to the Almighty Creator for allowing me to bring this effort into completion.

July 6, 2020

Abstract

QUANTIFYING SHALLOW DEPTH CONCRETE

DELAMINATIONS USING IMPACT ECHO

Mantaka Mahjabin Momo, MS

The University of Texas at Arlington, 2020

Supervising Professor: Nur Yazdani

Delamination is a type of deterioration commonly found in concrete structures. It may form due to corrosion of embedded steel, poor construction, excessive vibration, or lack of bonding in composite construction. Impact echo (IE) is a simple and straightforward non-destructive testing (NDT) technique that is used to detect the presence and extent of delamination within concrete structures. It is capable of detecting its presence of delaminations in deep depths, but cannot accurately measure the defects that are near the surface. This phenomenon occurs due to the differences in the vibration modes of deep and shallow depth delaminations.

The objective of this study was to quantify the depth of shallow depth delaminations, using the IE method. Four slab samples containing 12 near- surface delaminations were cast, and the impact echo test was performed on each of them. Frequency contour maps were drawn for each slab from which the average frequency of each delamination was determined. A numerical formulation that

correlated the average vibration response over the delaminated region, obtained from the IE test, and the geometry of the delaminations was suggested, based on the theoretical solution of flexural mode of vibration of thin rectangular plates. Regression analysis was performed for three selected dimensional parameters, and six regression functions (three logarithmic and three exponential) were suggested. The depths of the delaminations were predicted with these functions. It was observed that the exponential function correlating the flexural mode of vibration and the perimeter-to-depth ratio yielded the smallest percentage error in predicting the depths. As a result, this exponential equation was finalized as the flexural mode vibration equation for shallow depth delaminations, and recommendations for further work were suggested.

Table of Contents

List of Illustrations

List of Tables

Chapter 1

Introduction

Concrete highway bridges are continuously exposed to traffic and fluctuating weather conditions, and their deck slabs are the most susceptible of their components to deterioration, as they are directly exposed to traffic loading, as well as to various environmental conditions (e.g., thermal variations, rainfall, snow, etc.). One of the most common forms of deterioration is corrosion-induced deck delamination, which is depicted in Figure 1-1.

Figure 1-1 Significant bottom delamination

The predominant causes of corrosion are water and de-icing salt. In the southern regions of the United States, rainfall is very common, and in the northern regions, deicing salt is used to clear snow and ice from highways and bridges. The corrosion process starts when water and deicing salt penetrate the concrete through micro cracks and come in contact with the embedded rebar. The volume of the rebar expands, due to corrosion, and creates a subsurface fracture plane in the surrounding concrete that may extend upwards considerably, creating a substantial delaminated region within the structure (Shokouhi 2006, Gucunski et al. 2012). In composite construction, delamination may occur between the interfaces due to the loss of composite action. Poor construction and excessive vibration can also lead to the formation of delamination within the depths of the structure, thus decreasing its structural integrity. The creation and progression of this type of deterioration are not visible on the concrete surface, but if proper remedial steps are not taken in time, the delamination can lead to the formation of open spalls that will ultimately affect the structural integrity. The challenge lies in detecting the delamination in its early stages since it is not visible on the concrete surface.

Problem Statement

Various nondestructive testing (NDT) techniques are being used to assess the condition of concrete structures today, and the impact echo (IE) is one that is being used to detect internal defects within concrete. This method is based on the progression and reflection of body waves and can be used to detect the presence of wave reflectors such as delamination, voids, cracks, honeycombs, etc. within

the depths of structures. The contour image produced from this method is a good predictor of the location of deep and shallow defects. One of the advantages of the IE method is that it is not affected by weather conditions. The data acquisition consists of a simple test setup followed by straightforward data analysis; therefore, high efficiency in collecting the data is encouraged, but not mandatory.

The IE method is based on the thickness mode frequency and only depends on the depth of two reflecting surfaces, along with the velocity of the stress waves within the test material. For this reason this method is effective in accurately determining the thickness of structural members, as well as the depth of defects. In case of bridge decks, deep delaminations mainly occurs around the mid span while the shallow depth defects can be found at the support zone due to the development of negative moment. In shallow depth defects, the vibration mode changes, and the flexural mode vibration becomes dominant. The relationship for this mode is not as straightforward as the thickness mode of vibration, and as a result, the thickness found from the IE method for near-surface defects is inaccurate. Fortunately, the presence of such defects can be predicted qualitatively, but this limitation means that an overall quantitative evaluation of structures cannot be done using the IE method.

Objective

As mentioned in the previous section, the depth of near-surface defects cannot be determined by using the impact echo method. The main objective of this study is to address this limitation and bridge the knowledge gap in this area. The specific objectives of this study are to:

a) Analyze the impact echo test data collected for concrete slabs containing shallow depth delamination, and
b) Propose an analytical equation to quantify the depth of near-surface defects.

Organization

Chapter one provides a brief overview of the work and the objective behind it.

Chapter two contains a background review of the impact echo technique, and provides information derived from previous studies that were conducted to interpret the vibration behavior of the region that is above shallow depth delamination, using the impact echo technique.

Chapter three describes the design and subsequent preparation of the specimens.

Chapter four presents information regarding the impact echo test instrumentation and the experimental procedure. A brief overview on data collection is also provided in this chapter.

Chapter five provides a detailed discussion of the data analysis of the data sets that were obtained from the impact echo test.

Chapter six provides a summary of the research findings, along with recommendations for future work.

Chapter 2

Background

This section provides a brief review of the materials on which this research was conducted. A detailed literature review was performed on the fundamentals of the impact echo method, and the flexural mode of the vibration of thin plates was reviewed to interpret the vibration response that is due to the presence of shallow depth delamination.

Impact Echo (IE)

Historical background

Nondestructive testing (NDT) plays an important role in assessing the condition of structures and is a core research area in the National Institute of Standards and Technology (NIST), formerly known as the National Bureau of Standards (NBS). During the late 1970s, NBS investigated two major construction failures (Carino et al. 1983) and concluded that the in-place concrete strength was a contributing factor to these accidents. This event prompted them to undertake a long-term research program to evaluate the in-place characteristics of concrete. The first step taken in their research was to estimate the strength of concrete that developed during construction. Then their focus shifted towards detecting internal defects, and a test method based on stress waves was adopted, as stress wave propagation within solids is affected by its mechanical properties. The technique adopted later became known as the impact echo method. (Carino 2001),

IE method

Impact echo (IE) is a widely used non-destructive testing (NDT) method in which surface motion generated from a short duration impact is monitored to detect internal defects within structures. The short duration mechanical impact introduces a transient stress pulse that propagates through the solid as three types of stress waves, namely P wave, S wave and R wave. Both the P and S waves have a spherical wave front and are associated with normal stress and shear stress, respectively. On the other hand, the R wave is a surface wave that travels along the surface, away from the impact point (Carino 2001). The schematic diagram of these waves are shown in Figure 2-1**Error! Reference source not found.**.

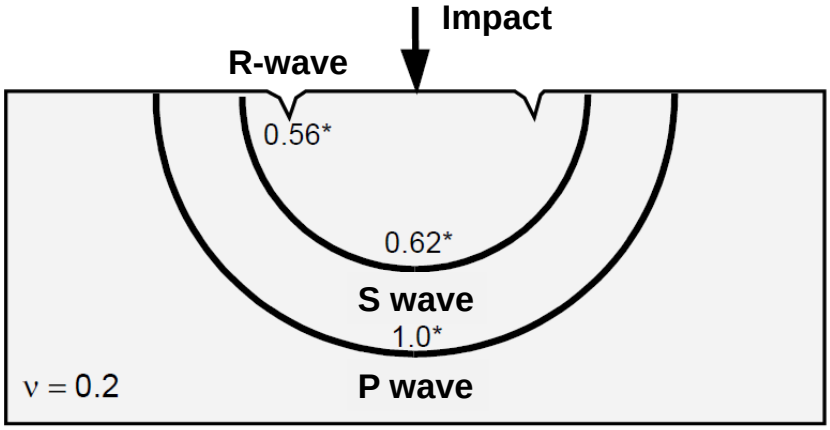

Figure 2-1 Stress waves in concrete plate due to an impact on the surface (Carino 2001)

Wave Propagation

When an impact is applied on the test surface, the progressing P and S waves travel through the depth of the plate and are reflected from the external

boundaries and the internal defects of the structure and return to the impacting surface. The arriving waves are again reflected by the free surface and propagate through the test object and are reflected by the internal defects and the external boundaries. These multiple reflected waves ultimately lead to the development of a transient resonance condition within the structure. The resulting surface displacement produced by the reflected body waves can be monitored by placing a receiving transducer close to the impact point, as shown in Figure 2-2. In such condition, the response is dominated by P wave echoes, as the displacements caused by P waves are larger than those caused by S waves at points near the impact point (Carino 2001, Carino and Sansalone 1990, Cheng and Sansalone 1993a, Sansalone and Carino 1986a).

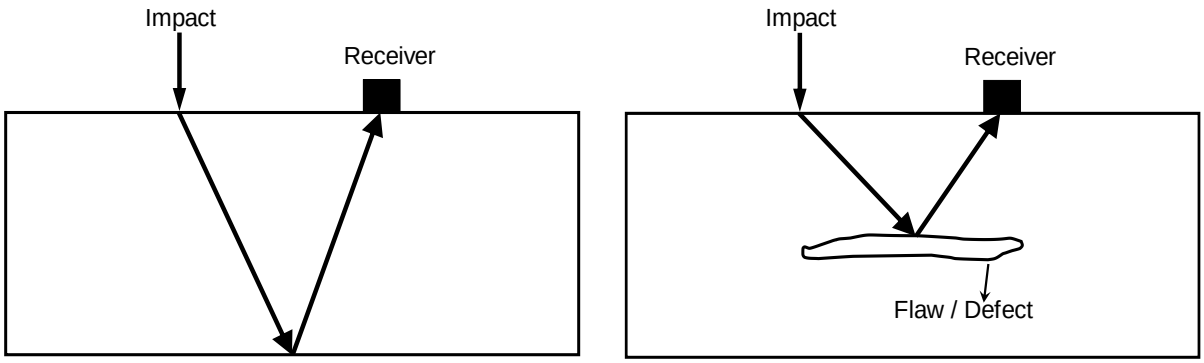

Figure 2-2 Wave reflection from (a) external boundary and (b) internal defects

If the thickness of the test surface and reflecting surface is T, the round-trip travel distance for the P wave can be considered as 2T. In such case, the frequency of P wave can be expressed as (Carino 2001):

$$f = \frac{C_{PP}}{2T} \quad \text{2-1}$$

Where:

T = Thickness of reflecting surface

C_P = Velocity of P wave

C_{PP} $= 0.96C_P$ (Lin and Sansalone 1997)

f = Thickness frequency

Equation 2-1 is the basic relationship for the interpretation of the impact echo test results.

Frequency Analysis

In the past, time domain analysis was used to measure the arrival time of the P wave after the impact was applied. This analysis is feasible, but it is time consuming and requires a significant level of skill. Frequency analysis became a substitute for time domain analysis and was a key tool in the development of the impact echo method. In frequency analysis, the recorded time domain signal is converted to a frequency domain, using the fast Fourier transform (FFT) technique, and the transformation results in the formation of an amplitude spectrum. For plate-like structures, the frequency associated with the peak of the amplitude spectrum is the thickness frequency (Carino 2001), and the value of the peak frequency can be used to determine the thickness of the reflecting interface, T, by expressing Equation 2-1 as:

$$T = \frac{C_{PP}}{2f} \quad \text{2-2}$$

American Society for Testing and Materials (ASTM) Test Method C 1383-15

The test standard followed for conducting an impact echo test is ASTM C 1383-15 (2015). ASTM Test Method C 1383 includes two procedures: Procedure A and Procedure B. Procedure A involves the determination of the P wave speed, which is accomplished by measuring the travel time of the P wave between two transducers placed at a known distance. Procedure B determines the thickness frequency, using the impact echo method, from which the plate thickness can be calculated from the previously determined P wave speed and the corresponding equations. A factor of 0.96 is multiplied by the wave speed determined from Procedure A because previous studies suggested that the apparent wave speed relating the thickness frequency and the plate thickness is approximately 96% of the P-wave speed (Lin and Sansalone 1997).

Deep and shallow delaminations

In the presence of deep delamination, the impact echo response is dominated by the P wave reflection from the surface of the delamination. The resulting waveform also shows the periodic displacement due to the reflection of the P wave, where the dominating mode of vibration is the thickness mode. The resulting amplitude spectrum typically contains a single peak, and the frequency (f) associated with this peak can be incorporated into Equation 2-2 to determine the depth of delamination.

On the other hand, the flexural mode of vibration dominates the impact echo response of the region over the near-surface defects or shallow delamination. This mode represents the out-of-plane vibration of thin the plate above the

delamination. This mode of vibration is fundamentally different from the thickness mode; therefore, the response cannot be interpreted using Equation 2-1 or 2-2. The frequency associated with the flexural mode depends on many factors, such as the lateral dimensions, depth, material properties, and boundary conditions of the delaminated section (Kee and Gucunski 2016). In the amplitude spectrum, the frequency peak for the flexural mode can be detected at a frequency lower than the thickness mode. By filtering out these low frequencies, the possible area for shallow depth delamination can be detected, although the depth remains unknown.

Interpretation of Shallow Depth Delamination with IE

As mentioned earlier, the impact echo method cannot interpret the vibration above shallow depth delaminations. Several studies have been performed to predict the vibration response for the region above defects that are near the surface, and the following section provides an overview of them.

A study by Cheng and Sansalone (1993a) proposed an analytical model to predict the vibration response for shallow depth delamination. Numerical analysis was performed, and the results were compared with the theoretical solution of thick rectangular plate vibration with a simply supported boundary condition on all four edges (Mindlin et al. 1956). The fundamental flexural frequency for the shallow depth delamination was found to be higher than the theoretical solution, and it was reasoned that the boundary conditions of the delaminated section are more rigid than the simply supported one, causing a higher flexural frequency. It was also deduced from this study that the fundamental flexural frequency of rectangular delamination in plates depends on the geometry (lateral dimensions and depth) of

the delamination as well as the material properties (modulus of elasticity, Poisson's ratio and density) of the plate. Another significant finding was that the vibration behavior could not be predicted by the theory of flexural vibration of the plate with increasing depth of delamination. On the basis of this observation, it was concluded that the delaminated region over a thick plate is too stiff to excite the flexural mode of vibration, and the thickness mode frequency is adequate for interpreting the vibration of the delaminated section.

Another study deduced that the response above a shallow depth delamination lies between the simply supported and clamped boundary conditions of classical thin plate vibrations (Oh et al 2013b). A classic analytical approach to determining the vibration modes of plates with semi-clamped boundary conditions can be challenging, so the researchers added an edge effect with a correction function to the classic solution of the thin rectangular plate vibration with simply supported boundary condition. The concept of the edge effect was used to account for the modified semi-clamped boundary condition. This study was performed for a width-to-depth ratio greater than 5.

One of the most recent studies was done by Kee and Gucunski (2016), where a semi-analytical formulation was proposed, based on the natural frequency of thin plate vibration with a simply supported boundary condition. In this study, the rectangular delaminated area was converted into an equivalent square with the size 'c'. This dimension was later used as the geometric property of the delamination, along with the depth in the proposed semi-analytical expression. This study suggested that the edge effect increases as the width-to-depth ratio

(c/h) decreases, and that it is more prominent for c/h<5. One of the aspects of this study was to determine the dimensions of the equivalent square delamination in order to develop a 2D visualization scheme. The depth of the delamination was a known parameter in this case, but in a practical case scenario, both the geometry and depth would be unknown. Therefore, the proposed model needs to be modified.

Chapter 3

Experimental Design and Sample Preparation

Reinforced concrete slabs were cast with artificial delaminations placed within the slabs at shallow depths. This section details the information on the planning and preparation of the sample slabs.

Specimen Design

Four reinforced concrete slabs with lateral dimensions of 4 ft x 4 ft (1.2 m x 1.2 m) were prepared for this research. The schematic diagrams of the slabs are presented in **Error! Reference source not found.** and **Error! Reference source not found.**.

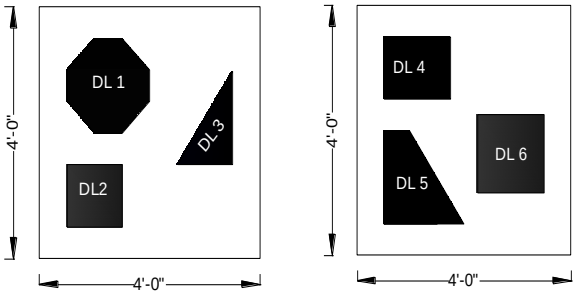

(a) Slab 1 (b) Slab 2

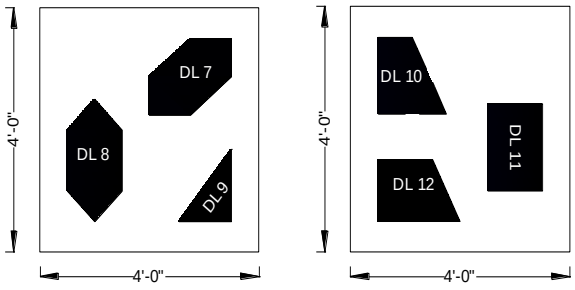

(c) Slab 3 (d) Slab 4

Figure 3-1 Plan view of the slabs showing the position of the delaminations

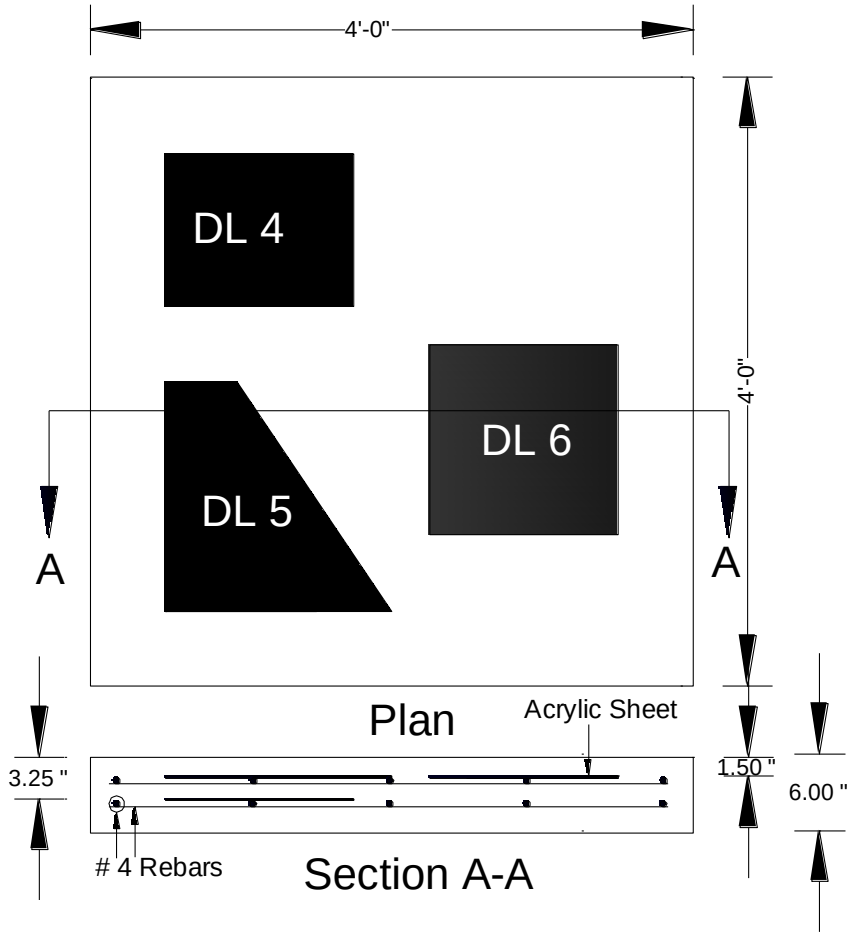

Figure 3-2 Delaminations placed at two depths

The thickness of the slabs was chosen as 6 in (15 cm) to accommodate the delaminations at two levels, within a 4 in (10 cm) depth. It was reported in the Impact Echo User Manual (2001) that the depth of the delaminations needs to be less than 4 in (10 cm) to excite the flexural mode of vibration. Consequently, the

thickness of the slabs was selected so that all of the delaminations could remain in the shallow regions.

Table 3-1 Detailed information of the prefabricated delaminations

Delamination	Area in^2 (mm^2)	Perimeter in (mm)	Depth in (mm)
DL1	252 (162580)	58 (1473)	3.25 (83)
DL2	144 (92903)	48 (1219)	1.5 (38)
DL3	106.5 (68710)	51.18 (1300)	1.5 (38)
DL4	180 (116129)	54 (1372)	3.25 (83)
DL5	213.75 (137903)	63.52 (1613)	1.5 (38)
DL6	225 (145161)	60 (1524)	1.5 (38)
DL7	216 (139355)	57.64 (1464)	3.25 (83)
DL8	216 (139355)	58 (1473)	1.5 (38)
DL9	85.92 (55432)	45.14 (1147)	1.5 (38)
DL10	165 (106451)	53.55 (1360)	3.25 (83)
DL11	193.375 (124758)	56.75 (1441)	1.5 (38)
DL12	175.83 (113438)	55.075 (1399)	1.5 (38)

Specimens Preparation

Four plywood formworks with dimensions of 4 ft x 4 ft x 0.5 ft (120 cm x 120 cm x 15 cm) were constructed. The delaminations were simulated with acrylic

sheets covered with two layers of plastic sheeting. This simulation was done to create a discontinuity within the depth of the slabs. The prefabricated delaminations were placed at two levels, depths of 1.5 in (38 mm) and 3.25 in (83 mm). To facilitate the placement of the delaminations, #4 (12.7 mm) rebars were provided in two directions at two levels. The complete formwork setup is shown in Figure 3-3.

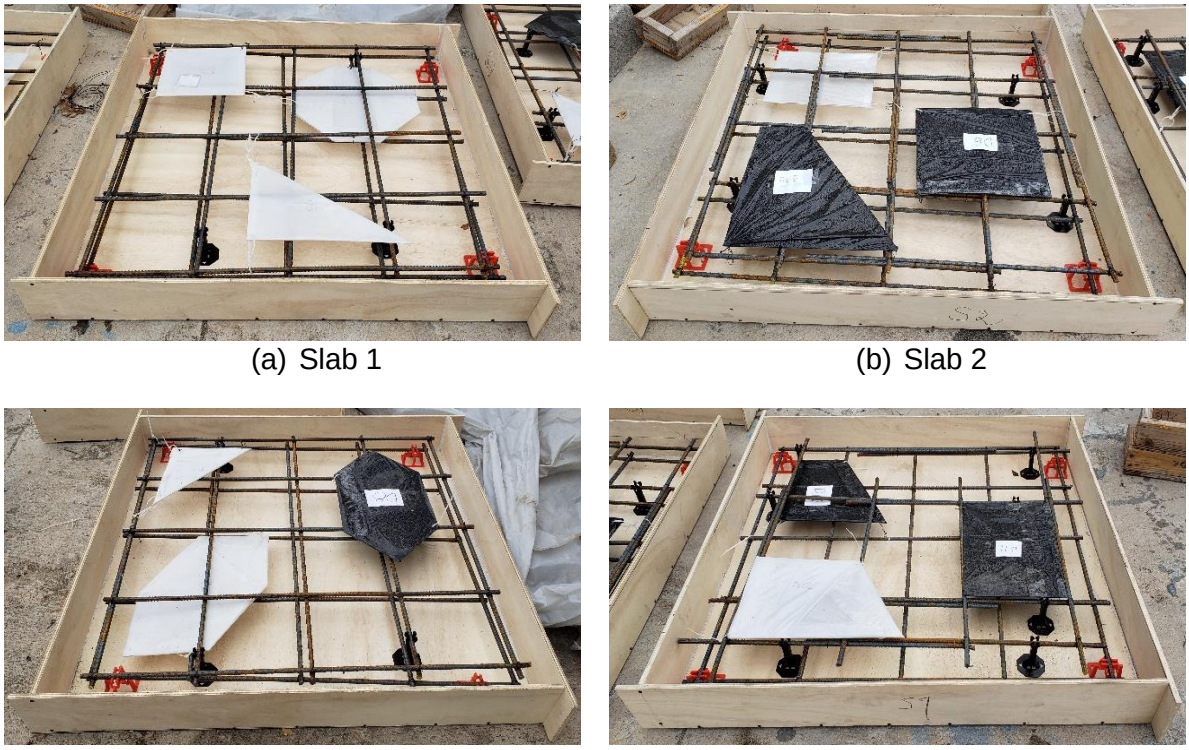

(a) Slab 1 (b) Slab 2

(c) Slab 3 (d) Slab 4

Figure 3-3 Formwork preparation and delamination placement

After preparing the formworks and placing the delaminations, the concrete slabs were cast, using a single batch of ready mix concrete. The slabs were sprayed with curing compound, the tops of the slabs were covered with a plastic sheet, and they were cured for 28 days to attain the target compressive strength

of 3000 psi (20.7 MPa). The material proportion of the concrete mix is shown in **Error! Not a valid bookmark self-reference.**. Casting of the slabs is shown in

(a) (b) (c) (d)

Figure 3-4. The slump of the concrete mix was 8 in (200 mm).

Table 3-2 Concrete material properties

Material	lb/ft^3 (kg/m^3)
Cement	12.5 (201)
Fly Ash	3.2 (51)
Water	8.8 (141)
Coarse aggregate	68.5 (1098)
Fine aggregate (Bristol sand)	13.3 (214)
Fine aggregate (Bridgeport sand)	40.0 (640)

(a) (b)

(c) (d)

Figure 3-4 Casting of the slabs: (a) formwork placement, (b) concrete pouring, (c) levelling top surface and (d) cast slabs

Chapter 4

Experimental Procedure and Data Collection

This section provides information on the impact echo scanning of the slabs and the corresponding data collection. A brief description of the instrumentation is provided in this chapter.

Impact Echo Instrumentation

The impact echo (IE) test method is a mechanical-wave-based non-destructive testing method in which an impact is applied on each testing point of the specimen surface. The corresponding vibration response is obtained via a transducer, and the time domain signal is converted into a frequency domain. The corresponding peak frequency provides information on the location of the flaw(s) within the specimen at that point. The testing points can be defined by drawing grid lines on the test surface.

The impact echo test setup is comprised of three basic components, namely the impactor, the transducer or receiver, and the data acquisition system. In this study, the NDE 360 system from Olson Instruments was used to conduct the impact echo test. The complete NDE 360 system consists of an IE test head and an NDE 360 platform, as shown in **Error! Reference source not found.**.

The IE test head has an automated solenoid impactor and a built-in transducer, as presented in Figure 4-2. The NDE 360 platform works as a data acquisition system. It is connected to the IE test head with an IE test cable. Impact can be applied on the test surface with the solenoid impactor after it has been

activated by the NDE 360 platform. This platform processes the data acquired from the transducer and displays the analyzed data on the screen.

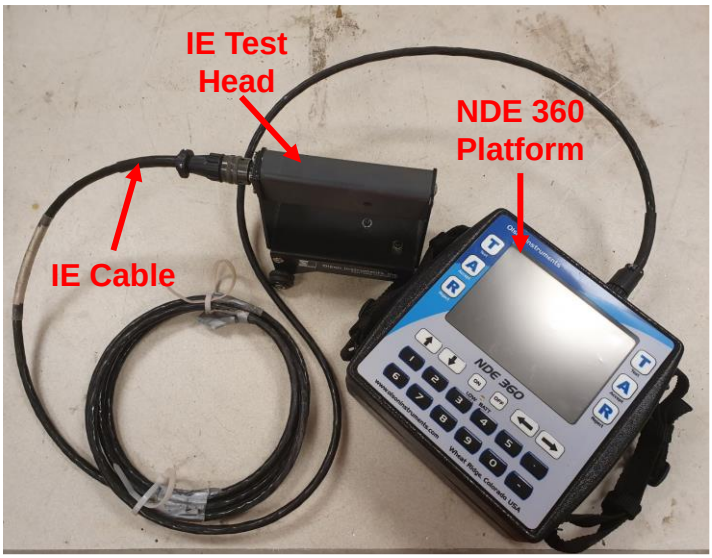

Figure 4-1 Major components of NDE 360 system

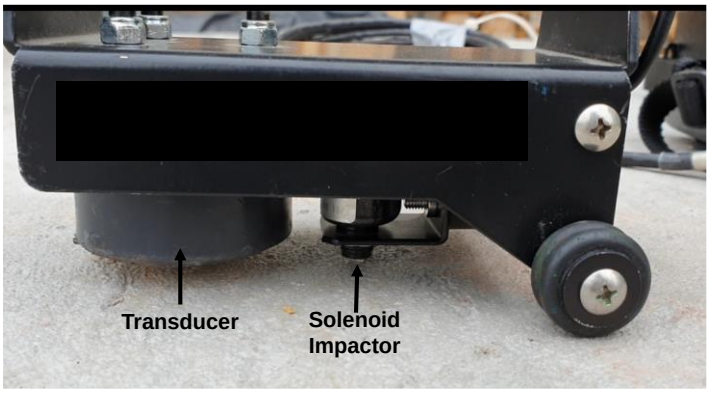

Figure 4-2 IE Test head components

Experimental Procedure

A grid size of 6 in x 6 in (15 cm x 15 cm) was selected for conducting the impact echo test. Chalk was used to draw the grids on the slabs, as shown in Figure 4-3.

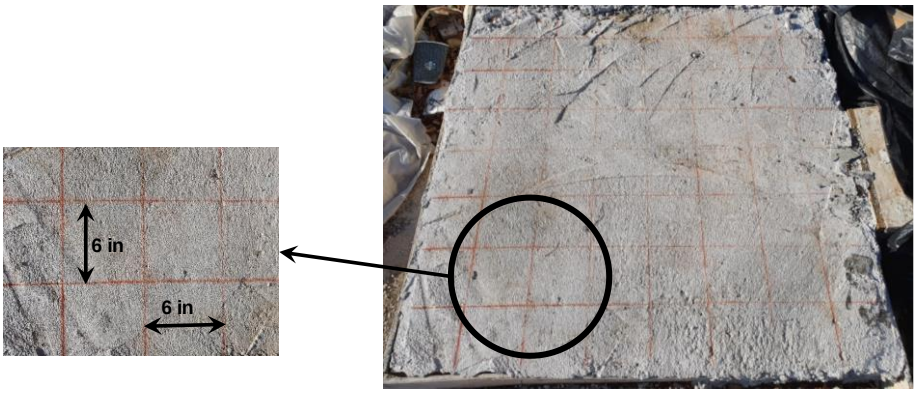

Figure 4-3 Grid lines on the slab

The IE test head was pressed firmly onto the test surface to ensure contact between the test head and the concrete surface in order to collect the impact echo test data. The solenoid impactor was placed directly above each grid point, the impact was applied, and the corresponding vibration response was processed with the NDE 360 platform. A compact flash drive was inserted into the NDE 360 platform to store the vibration response of all of the grid points. The stored data sets were further analyzed with WinIE software (Olson Instruments Inc, 2016) to obtain the peak frequencies.

Data Collection

The first step of data collection was the determination of the P wave velocity within the concrete structure. Velocity calibration can be done with the NDE 360 system for a region of known thickness, but the data can be collected without velocity calibration. In that case, the data sets are collected with a default P wave velocity of 12000 ft/s (3657.6 m/s).

The impact echo test was conducted near the slab edge to determine the P wave velocity. The location near the slab edge was selected because there was

no delamination within that region, so a known thickness of 6 in (15 cm) could be provided as input for the NDE 360 platform. The collected data was processed in WinIE software (Olson Instruments Inc, 2016), and the result is shown in Figure 4-4. The velocity of the P wave obtained from the software was 10603 ft/s (3232 m/s).

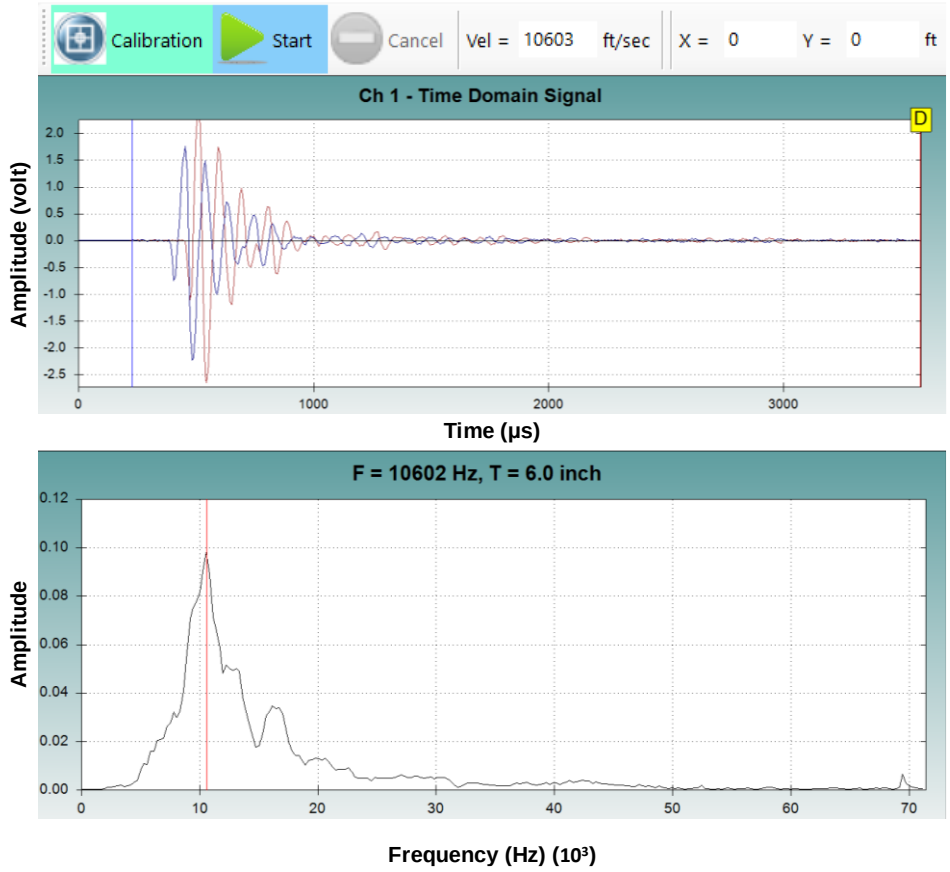

Figure 4-4 Velocity Calibration in WinIE Software

The output from WinIE (Olson Instruments Inc, 2016) software contains the time domain signal (amplitude vs time) and the amplitude spectrum (amplitude vs frequency). The amplitude spectrum is obtained from the fast Fourier transform of

the time domain signal. The amplitude spectrum is obtained from the peak frequency.

After determining the velocity of the P wave, the impact echo test was conducted on each predefined grid point. The collected data sets were further analyzed in WinIE software (Olson Instruments Inc, 2016) to obtain the peak vibration frequencies for the corresponding points.

Chapter 5

Data Analysis

The collected data sets were further processed to develop the frequency contour maps from which the average frequencies for the delaminations were determined. After that, regression analysis was performed to express the parameters in terms of a mathematical correlation.

Frequency Contour Map

The first step of the data analysis was to produce frequency contour maps for the slabs, using the Surfer Student v18 software (Golden Software, LLC 2020). The frequency contour maps of the four slabs, along with the locations of the delaminations, are presented in **Error! Reference source not found.**. It can be observed that the frequencies were concentrated within the boundaries of the delaminations. Two types of frequency-concentrated regions are apparent in **Error! Reference source not found.**: the high frequency zone (red) and the low frequency zone (blue). The delaminations at 3.25 in (83 mm) depth are located in the red region and the ones at 1.5 in (38 mm) depth are in the blue region. From this observation it can be concluded that frequency contour maps clearly distinguish delaminations at both deep and shallow depths.

The next step was to determine the average frequency for each delamination. The frequency volumes within the boundaries of the delaminations were obtained from the Surfer software, and the volume was divided by the corresponding planar area of the delamination to get the weighted average

frequency of the corresponding delamination. The weighted average frequencies thus determined were utilized in the data analysis.

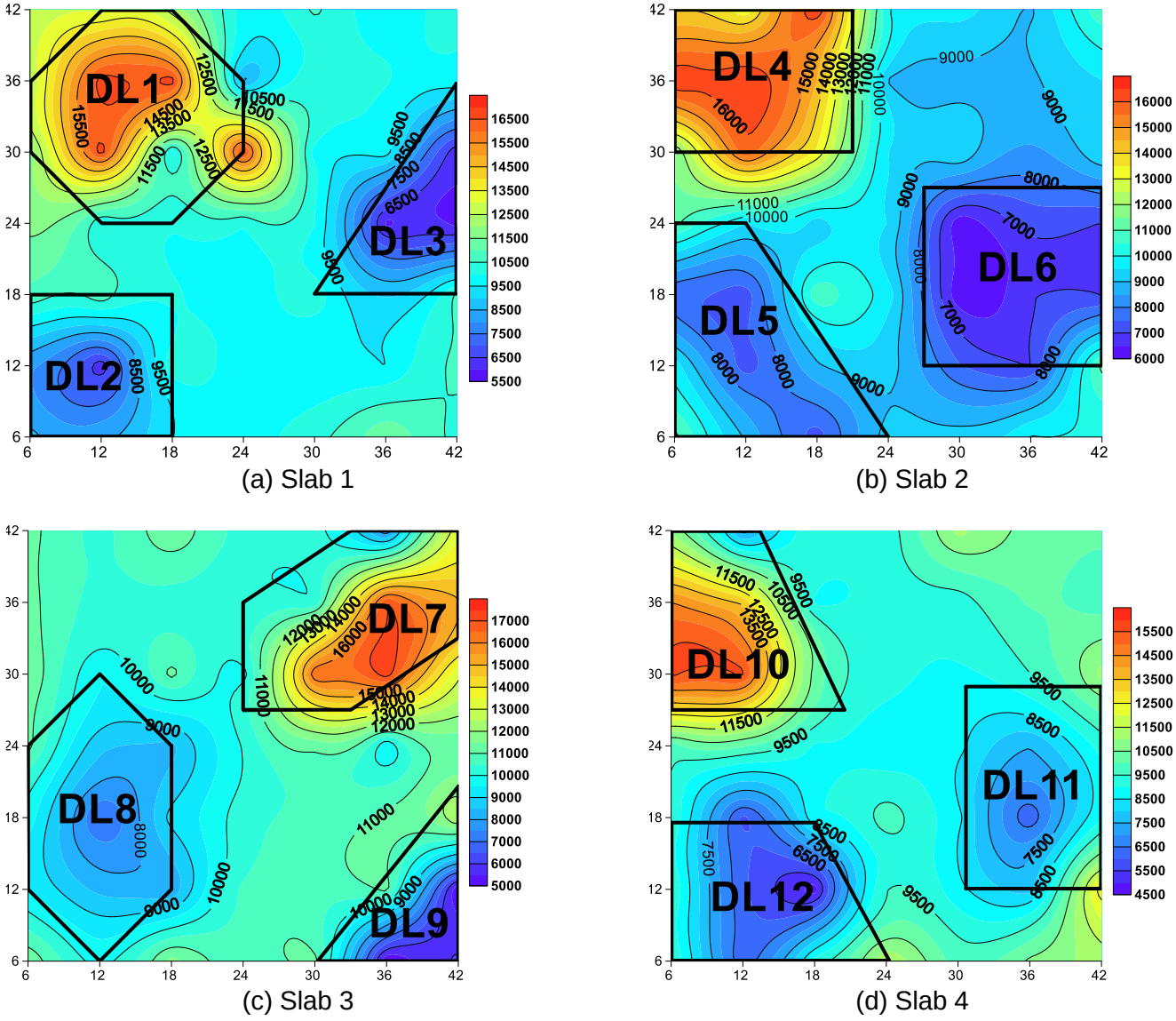

(a) Slab 1

(b) Slab 2

(c) Slab 3

(d) Slab 4

Figure 5-1 Frequency contour maps of four slabs (axis dimensions in inches)

Proposed Frequency Equation

Before proceeding with the regression analysis, parameters were selected, based on the proposed mathematical expression for the flexural mode of vibration.

The proposed equation aimed at characterizing the flexural mode of vibration over a delaminated region. This suggested formulation was based on the flexural mode vibration of thin plate. The classical solution for the fundamental natural frequency of a thin plate with simply supported boundary condition can be expressed by Equation **Error! Reference source not found.** (Mitchel and Hazell 1987).

$$f = \frac{\pi}{2}\left(\frac{1}{a^2}+\frac{1}{b^2}\right)\sqrt{\frac{D}{\rho h}} \qquad 5\text{-}1$$

Where:

$a, b =$ Length and width of rectangular plate

$\mathrm{E} =$ Young's modulus

$\mathrm{D} =$ Flexural rigidity, $\frac{Eh^3}{12(1-\vartheta^2)}$

$\mathrm{h} =$ Thickness of the plate

$\rho =$ Mass density

$\vartheta =$ Poisson's ratio

As the boundary condition for the delaminated section is between the simply supported and clamped boundary conditions of thin plates, earlier studies (Oh et al. 2013b) introduced an edge effect factor into Equation **Error! Reference source not found.** to account for the semi-clamped boundary condition, which in

turn depends on the width-to-depth ratio of the rectangular plate. In practice, the delamination would have an arbitrary shape, and it would be difficult to choose a width that could be correlated to the edge effect. So rather than width, it would be more feasible to work with the perimeter and area of the delamination. Equation **Error! Reference source not found.** can rearranged as:

$$f = \frac{\pi}{2}\left(\frac{a^2 + b^2}{a^2 b^2}\right)\sqrt{\frac{D}{\rho h}}$$

$$\Rightarrow f = \frac{\pi}{2}\left(\frac{(a+b)^2 - 2ab}{a^2 b^2}\right)\sqrt{\frac{D}{\rho h}}$$

$$\Rightarrow f = \frac{\pi}{2A^2}\left(\frac{P^2}{4} - 2A\right)\sqrt{\frac{D}{\rho h}} \qquad 5\text{-}2$$

$$\Rightarrow f = C_{rec}^2 \frac{\pi}{2h^2}\sqrt{\frac{D}{\rho h}} \qquad 5\text{-}3$$

Where:

$P =$ Perimeter of rectangular plate

$A =$ Area of the rectangular plate

$C_{rec}^2 = \frac{h^2}{A^2}\left(\frac{P^2}{4} - 2A\right)$

In accordance with Equation 5-3, an analytical formulation for flexural mode vibration, f_{DL} for arbitrarily shaped delamination can be proposed as:

$$f_{DL} = C_{DL}^2 \frac{\pi}{2h^2}\sqrt{\frac{D}{\rho h}} \qquad 5\text{-}4$$

Here C_{DL}^2 is the dimensionless frequency that is introduced in Equation 5-4 to consider the mixed boundary condition, as well as the arbitrary shape and size of the delamiations. Equation 5-4 can be further expressed in terms of the parameters obtained from the impact echo test, as shown in Equation 5-5.

$$\text{P wave velocity}, C_p = \sqrt{\frac{E(1-\vartheta)}{\rho(1+\vartheta)(1-2\vartheta)}}\ ; (\text{Carino}, 2001)$$

$$\text{Flexural rigidity}, \text{D} = \frac{Eh^3}{12(1-\vartheta^2)}$$

$$f_{DL} = C_{DL}^2 \frac{\pi}{2h^2}\sqrt{\frac{D}{\rho h}} = C_{DL}^2 \frac{\pi}{h} \times \frac{C_p}{(1-\vartheta)}\sqrt{\frac{(1-2\vartheta)}{48}} \qquad 5\text{-}5$$

Regression Analysis

The objective of the regression analysis was to express the dimensionless frequency in Equation 5-5 in terms of some known parameters. Comparing Equation 5-3 and Equation 5-4 led to the assumption that the dimensionless frequency can be expressed as:

$$C_{DL}^2 = \text{f}\left(\frac{h}{b}\right) \qquad 5\text{-}6$$

Equation 5-6 expresses the dimensionless frequency as a function of a dimensionless parameter. Here, ‘b’ is a dimensional parameter that can be defined as:

$$\frac{1}{b^2} = \frac{1}{A^2}\left(\frac{P^2}{4} - 2A\right)$$

The average frequency for each delamination was determined from the contour map. The dimensionless frequency can be determined using Equation 5-7 for a known depth of delamination and frequency of vibration.

$$C_{DL}^2 = f_{DL} h \frac{(1-\vartheta)}{\pi C_p}\sqrt{\frac{48}{(1-2\vartheta)}} \qquad 5\text{-}7$$

The dimensionless frequency was also plotted against other parameters, and based on observations of their correlations, two additional parameters were selected for the regression analysis, as shown in Equation 5-8 and Equation 5-9.

$$C_{DL}^2 = \mathrm{f}\left(\frac{P}{h}\right) \qquad 5\text{-}8$$

$$C_{DL}^2 = \mathrm{f}\left(\frac{Ph}{A}\right) \qquad 5\text{-}9$$

The regression analysis was done using R software. It was observed that the correlations shown in Equations 5-6, 5-8 and 5-9 were best explained by logarithmic and exponential functions. Therefore, regression analysis was done for both the exponential and logarithmic functions of each of the three selected parameters. Both functions were converted into linear functions, and the linear regression analysis was done by using R software with the corresponding parameters. The default level of significance of 0.05 was used for the regression analysis. A summary of the results of the regression analysis, along with the regression functions, is shown in **Error! Reference source not found.**.

After performing the regression analysis, the coefficient of determination (R-squared value) was observed for each model to determine the goodness of fit. An R-squared value close to 1 can be interpreted as a better-fitted model. A comparison of the R-squared values in **Error! Reference source not found.** shows that the regression model represented by Equation 5-8 is the best-fitted model. For both the logarithmic and exponential models of this parameter, the coefficient of determination values are close to 1. Apart from the coefficient of determination, the F value and the p-value from the ANOVA table were observed to determine whether the regression functions were statistically significant. A statistically significant linear regression model is the one in which the F value is greater than 1 and the p-value is less than 0.05.

Table 5-1 Summary of regression analysis

Model	Equation from Analysis	R^2	F	p
$C_{DL}^2 = \begin{cases} \mathrm{f}\left(\frac{P}{\mathrm{h}}\right) \\ \mathrm{f}\left(\frac{\mathrm{h}}{b}\right) \\ \mathrm{f}\left(\frac{P\mathrm{h}}{A}\right) \end{cases}$	$\mathrm{f}\left(\frac{P}{h}\right) = 3.0681853 - 0.7851072 \times \ln\left(\frac{P}{h}\right)$	0.932	151.7	$2.287\text{x}10^{-7}$
	$\mathrm{f}\left(\frac{P}{h}\right) = 2.22e^{-0.060272\left(\frac{P}{h}\right)}$	0.8833	84.28	$3.46\text{x}10^{-6}$
	$\mathrm{f}\left(\frac{h}{b}\right) = 1.308150 + 0.574403 \times \ln\left(\frac{h}{b}\right)$	0.434	9.434	0.01181
	$f\left(\frac{h}{b}\right) = 0.106e^{5.19718\left(\frac{h}{b}\right)}$	0.4655	10.58	0.008677
	$\mathrm{f}\left(\frac{Ph}{A}\right) = 0.783072 + 0.6909847 \times \ln\left(\frac{Ph}{A}\right)$	0.6234	19.21	0.001371
	$\mathrm{f}\left(\frac{Ph}{A}\right) = 0.0816e^{2.293294\left(\frac{Ph}{A}\right)}$	0.6847	24.88	0.0005467

In accordance with the discussion, it can be concluded that the models shown in **Error! Reference source not found.** are statistically significant models, as all of them have a F value greater than 1 and a p-value less than 0.05.

Depth Prediction

The next step of the regression analysis was to predict the depth of the delaminations. The regression functions described in **Error! Reference source not found.** were individually plugged into Equation 5-5, and the depth of delamination was predicted using the trial and error method. The trial and error method was selected because it was more convenient than solving the equation.

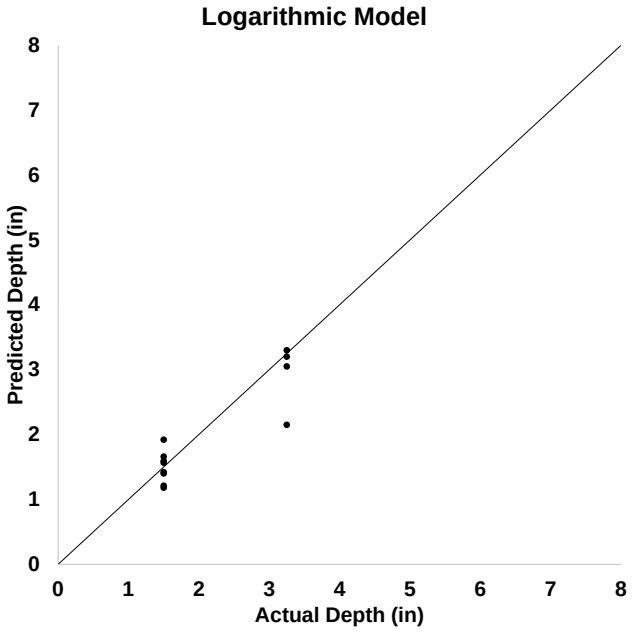

(a)

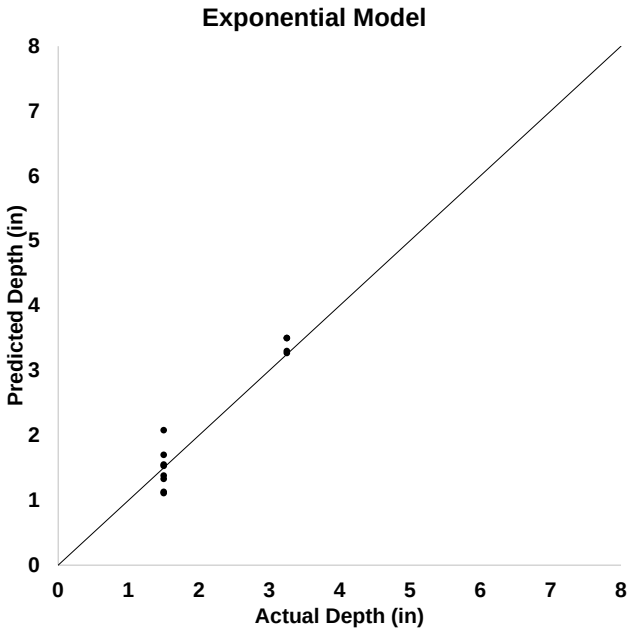

(b)

Figure 5-2 Actual depth vs predicted depth based on Equation 5-5 and 5-8 (a) logarithmic model (b) exponential model

The graphical representations of the predicted and actual depths, based on Equations 5-5 and 5-8, are presented in

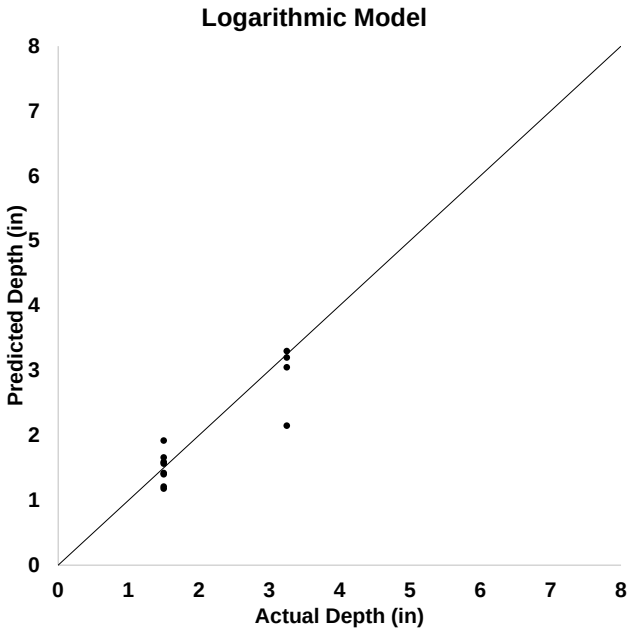
Logarithmic Model
Predicted Depth (in)
Actual Depth (in)
0
1
2
3
4
5
6
7
8

(a)

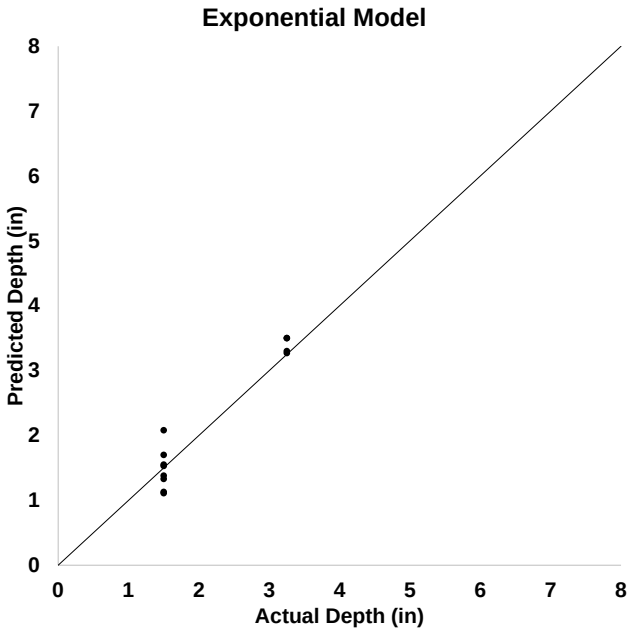
Exponential Model
Predicted Depth (in)
Actual Depth (in)
0
1
2
3
4
5
6
7
8

(b)

Figure 5-2. The predicted depths and the percentage errors for the corresponding regression functions are shown in **Error! Not a valid bookmark self-reference.**.

Table 5-2 Predicted depth based on Equation 5-5 and 5-8

Delamination	$f_{DL} = \mathrm{f}\left(\frac{P}{h}\right) \times \frac{\pi}{h} \times \frac{C_p}{(1-\vartheta)}\sqrt{\frac{(1-2\vartheta)}{48}}$					
	$\mathrm{f}\left(\frac{P}{h}\right) = 3.0681853 - 0.7851072 \times \ln\left(\frac{P}{h}\right)$			$\mathrm{f}\left(\frac{P}{h}\right) = 2.22e^{-0.060272\left(\frac{P}{h}\right)}$		
	Actual Depth (in)	Predicted Depth (in)	Error (%)	Actual Depth (in)	Predicted Depth (in)	Error (%)
DL1	3.25	3.20	-1.54	3.25	3.50	7.69
DL2	1.5	1.21	-19.27	1.5	1.11	-26.00
DL3	1.5	1.40	-6.67	1.5	1.38	-8.00
DL4	3.25	3.05	-6.15	3.25	3.30	1.54
DL5	1.5	1.92	28.00	1.5	2.00	33.3
DL6	1.5	1.59	6.00	1.5	1.53	2.00
DL7	3.25	3.30	1.54	3.25	3.50	7.69
DL8	1.5	1.66	10.67	1.5	1.70	13.33
DL9	1.5	1.18	-21.33	1.5	1.13	-24.67
DL10	3.25	2.15	-33.85	3.25	3.27	0.62
DL11	1.5	1.57	4.33	1.5	1.55	3.33
DL12	1.5	1.42	-5.33	1.5	1.33	-11.33

A comparison of the actual depth and predicted depth, based on Equations 5-5 and 5-9, is depicted in Figure 5-3, and the corresponding predicted depths and error percentages are presented in Table 5-3. Similar graphical and tabular representations were done for the proposed frequency equation, based on Equations 5-5 and 5-7 in Figure 5-4 and

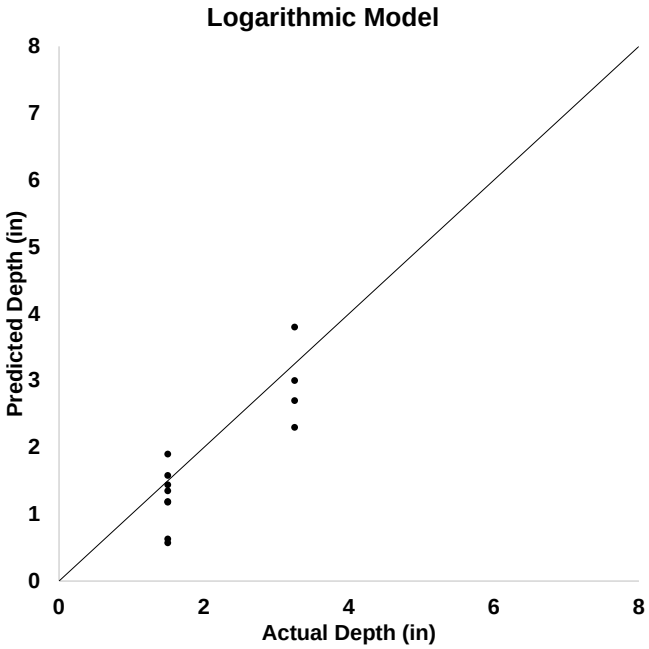
Logarithmic Model
Predicted Depth (in)
Actual Depth (in)
0
1
2
3
4
5
6
7
8

(a)

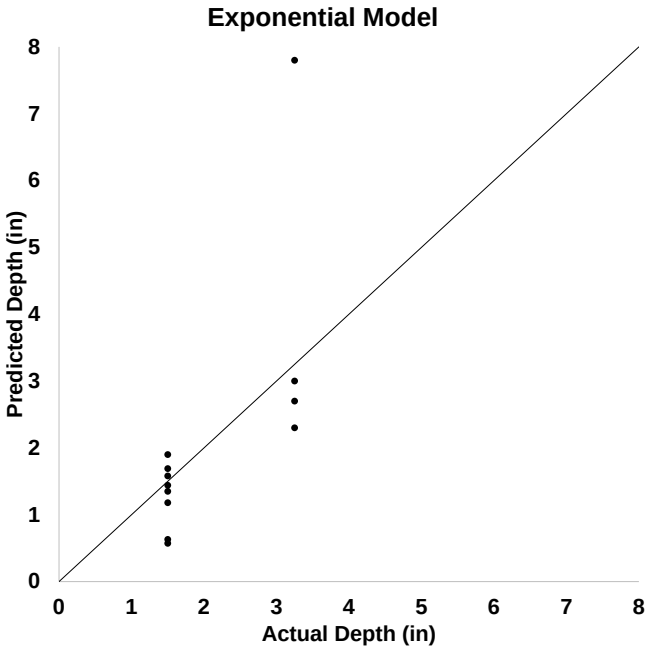
Exponential Model
Predicted Depth (in)
Actual Depth (in)
0
1
2
3
4
5
6
7
8

(b)

Figure 5-4 Actual depth vs predicted depth based on Equations 5-5 and 5-6 (a) logarithmic model (b) exponential model

Table 5-4, respectively.

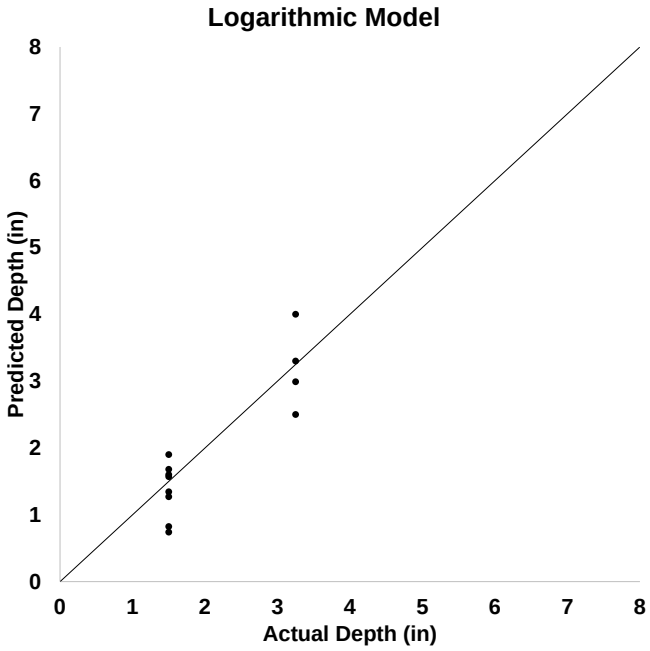

(a)

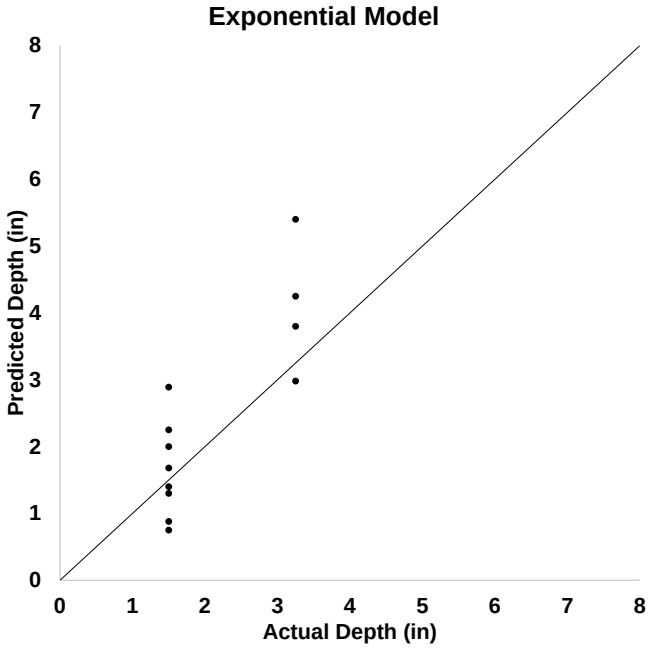

(b)

Figure 5-3 Actual depth vs predicted depth based on Equations 5-5 and 5-9 (a) logarithmic model (b) exponential model

Table 5-3 Predicted depth based on Equations 5-5 and 5-9

Delamination	$f_{DL} = \mathrm{f}\left(\frac{Ph}{A}\right) \times \frac{\pi}{h} \times \frac{C_p}{(1-\vartheta)}\sqrt{\frac{(1-2\vartheta)}{48}}$					
	$\mathrm{f}\left(\frac{Ph}{A}\right) = 0.783072 + 0.6909847 \times \ln\left(\frac{Ph}{A}\right)$			$\mathrm{f}\left(\frac{Ph}{A}\right) = 0.0816e^{2.293294\left(\frac{Ph}{A}\right)}$		
	Actual Depth (in)	Predicted Depth (in)	Error (%)	Actual Depth (in)	Predicted Depth (in)	Error (%)
DL1	3.25	4.00	23.08	3.25	5.40	66.15
DL2	1.5	1.27	-15.33	1.5	1.30	-13.33
DL3	1.5	0.82	-45.07	1.5	0.88	-41.33
DL4	3.25	2.99	-8.00	3.25	3.80	16.92
DL5	1.5	1.60	6.67	1.5	2.25	50.00
DL6	1.5	1.68	12.00	1.5	1.68	12.00
DL7	3.25	3.30	1.54	3.25	4.25	30.77

DL8	1.5	1.90	26.67	1.5	2.89	92.67
DL9	1.5	0.74	-50.67	1.5	0.75	-50.00
DL10	3.25	2.50	-23.08	3.25	2.98	-8.31
DL11	1.5	1.57	4.67	1.5	2.00	33.33
DL12	1.5	1.34	-10.40	1.5	1.40	-6.67

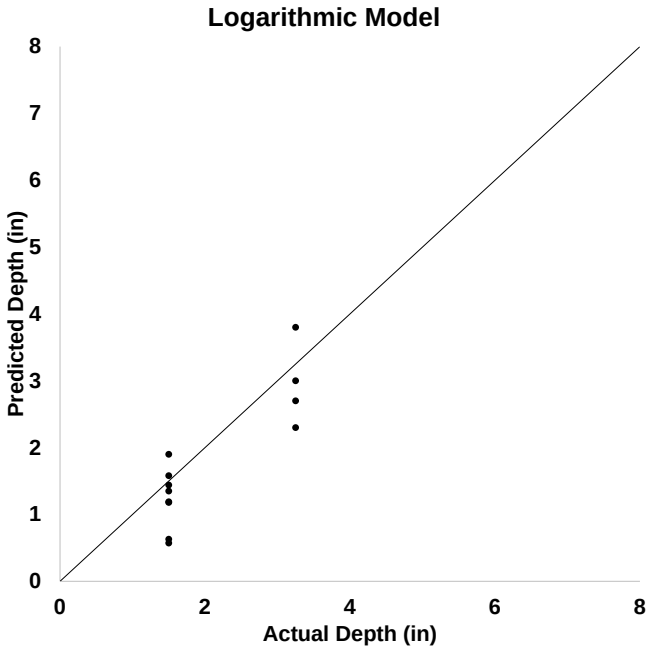

(a)

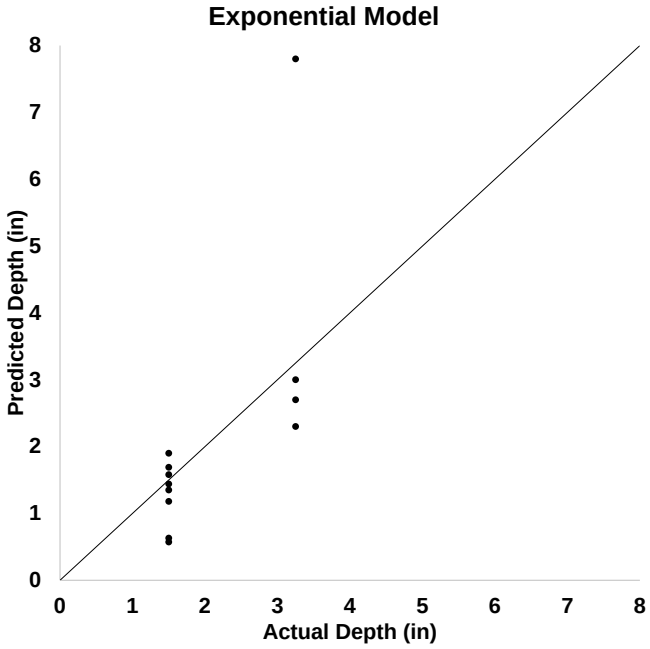

(b)

Figure 5-4 Actual depth vs predicted depth based on Equations 5-5 and 5-6 (a) logarithmic model (b) exponential model

Table 5-4 Predicted depth based on Equations 5-5 and 5-6

Delamination	$f_{DL} = \mathrm{f}\left(\frac{h}{b}\right) \times \frac{\pi}{h} \times \frac{C_p}{(1-\vartheta)} \sqrt{\frac{(1-2\vartheta)}{48}}$					
	$\mathrm{f}\left(\frac{h}{b}\right) = 1.308150 + 0.574403 \times \ln\left(\frac{h}{b}\right)$			$\mathrm{f}\left(\frac{h}{b}\right) = 0.106e^{5.19718\left(\frac{h}{b}\right)}$		
	Actual Depth (in)	Predicted Depth (in)	Error (%)	Actual Depth (in)	Predicted Depth (in)	Error (%)
DL1	3.25	3.80	16.92	3.25	7.80	140.00
DL2	1.5	1.18	-21.33	1.5	1.18	-21.33
DL3	1.5	0.63	-58.00	1.5	0.63	-58.00
DL4	3.25	2.70	-16.92	3.25	2.70	-16.92
DL5	1.5	1.35	-10.00	1.5	1.35	-10.00
DL6	1.5	1.58	5.33	1.5	1.58	5.33
DL7	3.25	3.00	-7.69	3.25	3.00	-7.69

DL8	1.5	1.90	26.67	1.5	1.90	26.67
DL9	1.5	0.57	-61.87	1.5	0.57	-61.87
DL10	3.25	2.30	-29.23	3.25	2.30	-29.23
DL11	1.5	1.44	-4.00	1.5	1.44	-4.00
DL12	1.5	1.19	-20.67	1.5	1.69	12.67

The solid lines in

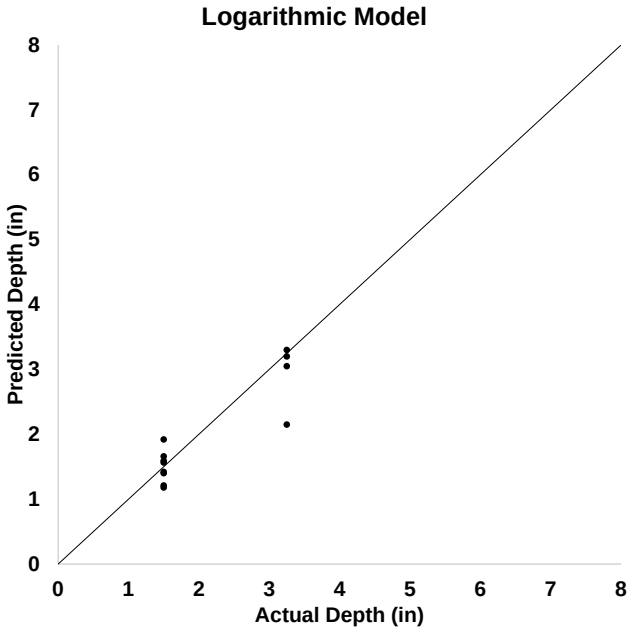

(a)

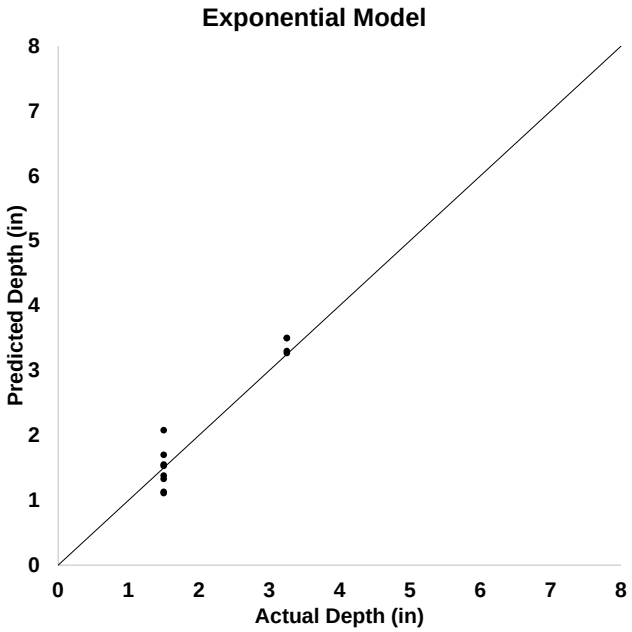

(b)

Figure 5-2, Figure 5-3 and Figure 5-4 represent the lines at which the predicted depth and the actual depth are equal. The points in

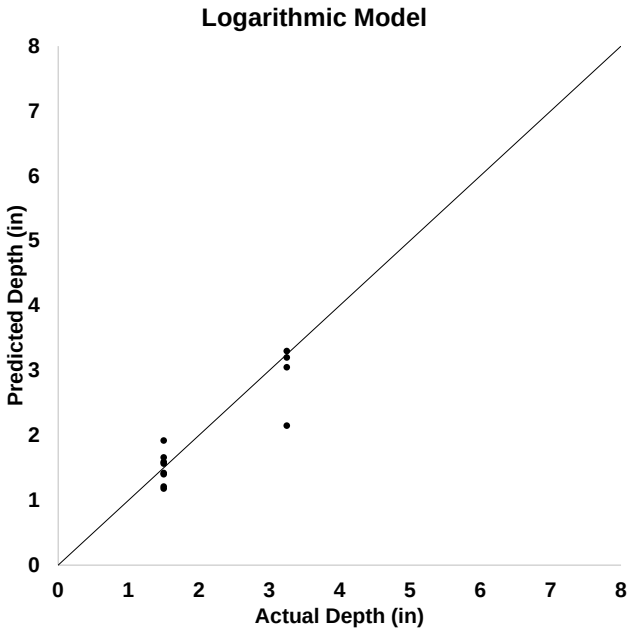

(a)

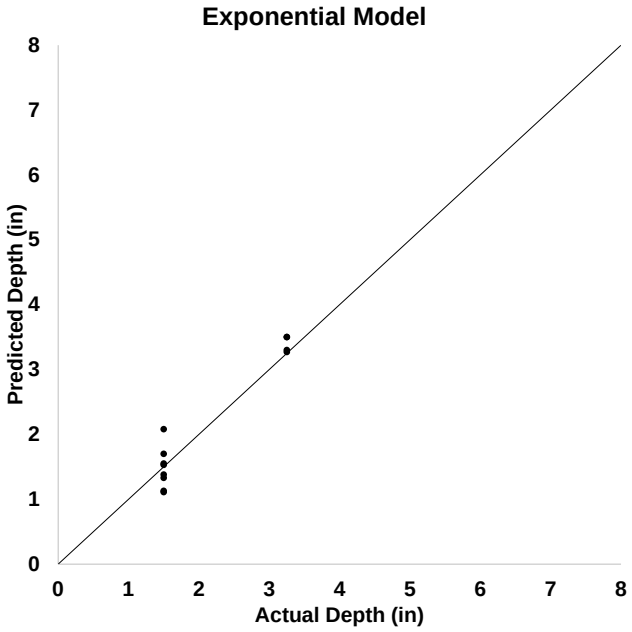

(b)

Figure 5-2 are more scattered around the solid line than the points in Figure 5-3 and Figure 5-4. From

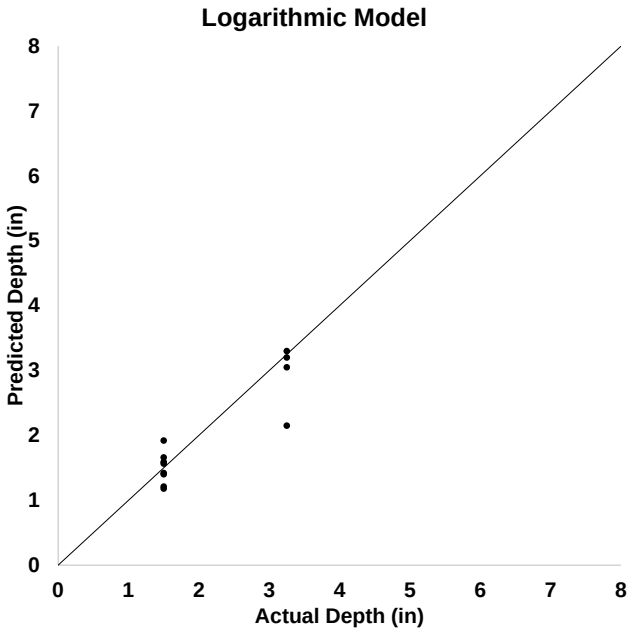

(a)

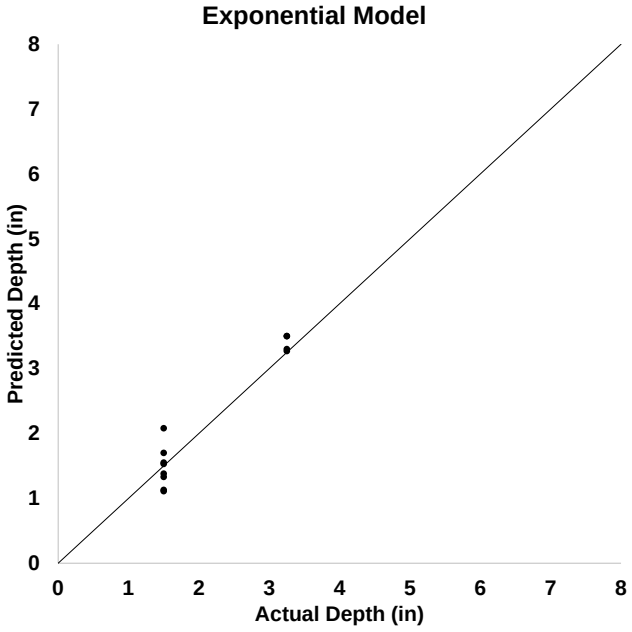

(b)

Figure 5-2 it can be observed that the data points in the exponential model are less scattered than in the logarithmic model. On the basis of these

observations, it can be concluded that the exponential model, based on Equations 5-5 and 5-8, is more appropriate for predicting the depth of shallow depth delamination. The selected flexural vibration equation can be expressed as:

$$f_{DL} = 2.22e^{-0.060272\left(\frac{P}{h}\right)} \times \frac{\pi}{h} \times \frac{C_p}{(1-\vartheta)}\sqrt{\frac{(1-2\vartheta)}{48}} \qquad 5\text{-}10$$

Although less error is observed for the selected exponential model, there are still three delaminations for which the percentage of error for the predicted and actual depth is greater than 20%. These three delaminations are DL2, DL5, and DL9. The high percentage of error for these three delaminations may be due to the collection of more data points around the edges and corners, as shown in Table 5-5.

Table 5-5 Location of IE data points

Delamination	Edge	Internal	Corner
DL1	8	4	8
DL2	8	1	4
DL3	5	1	2
DL4	7	2	2
DL5	7	3	3
DL6	5	4	2
DL7	4	4	1
DL8	8	3	6
DL9	5	1	2
DL10	4	3	1
DL11	4	2	1

DL12	5	2	1

Wave scattering attenuation may occur around the edges, and the IE signal may not be accurately interpreted close to the perimeter of the delaminated region (Kee and Gucunski 2016). Consequently, erroneous results may be noticed for these specific three delaminations.

Chapter 6

Conclusions and Recommendations

This chapter presents an overview of the results of the data analysis and the procedure followed in this study to obtain the depth of shallow depth delaminations. In addition, recommendations for further study are provided.

Research Findings

The aim of this study was to predict the depth of near-surface or shallow depth delaminations, based on the vibration response from the impact echo test. To achieve this objective, a numerical formulation was developed to correlate the geometry of the shallow depth delamination to the flexural mode of vibration. Four reinforced concrete slabs with prefabricated delaminations were cast, with all of the delaminations placed within the shallow depth region. Each slab contained three delaminations at two depth levels. Using the NDE 360 system, the impact echo test was conducted on each slab at the predefined grid points. The frequency data obtained from the IE test was processed with WinIE software, and frequency contour maps were drawn with Surfer software to obtain the average frequency of each delamination. A concentrated frequency in the locations of the delaminations was observed from the contour maps. A low frequency was obtained for the delaminations situated at shallower depths, and a higher frequency was obtained for the delaminations at deeper depths. Thus, it was necessary to depict the shallower and deeper depths of delamations in different colors. As a result, the

location of delaminations at two depth levels can be determined by the frequency contour maps

Although the location of the delaminations could be predicted from the frequency contour maps, the actual depth of the shallow depth delamination could not be obtained. The flexural mode of vibration is the vibration mode for shallow depth delamination and is fundamentally different from the thickness mode of vibration on which the conventional impact echo test was established. For this reason, a numerical formulation for the vibration of the shallow depth delamination was suggested, as shown in Equation 5-5. This equation was based on the theoretical solution of the flexural mode vibration of a thin rectangular plate. To account for the different boundary conditions and the shape and size of the delaminations, a parameter named dimensionless frequency was introduced in Equation 5-5. Regression analysis was performed to express this dimensionless frequency as a function of the dimensional parameters of the delaminations. Three dimensionless parameters were selected for this purpose, as prescribed in Equations 5-6, 5-8 and 5-9. For each of these parameters, logarithmic and exponential regression functions were established, as shown in Table 5-1. These six functions were plugged into Equation 5-5, and the depths were predicted for each of them. It was observed from the regression analysis that the exponential formulation between the fundamental peak frequency over the shallow depth delaminated region and the perimeter-to-depth ratio produced a smaller percentage of error. Therefore, the exponential correlation between the flexural

mode frequency and the perimeter-to-depth ratio, as shown in Equation 5-10, was selected to predict the depth of near-surface defects.

Recommendations for Future Research

In this research, only the vibration response over shallow depth delaminated regions was considered. The delaminations were placed at two depth levels, and the vibration response of each delamination was observed from the impact echo test results. The following are recommendations for further research on this topic.

- Two depth levels of delaminations were considered for this study. It is recommended that artificial delaminations be placed at more than two depth levels to further verify this research.
- It was noticed in this research that the impact echo test data sets collected from rough edges and corner points can produce erroneous results. To avoid this, circular delaminations or delaminations with curvature could be used for future research.
- Data sets collected from twelve delaminations were used for data analysis in this study. The number of delaminations can be increased to get a more refined result from the regression analysis.

References

ASTM (2015), “Standard Test Method for Measuring the P-Wave Speed and the Thickness of Concrete Plates Using the Impact-Echo Method.” ASTM C1383-15, West Conshohocken, PA, 2015.

Carino, N.J., Woodward, K.A., Leyendecker, E.V., and Fattal, S.G., (1983). “A Review of the Skyline Plaza Collapse.” *Concrete International*, Vol. 5, No. 7, July, pp 35-42.

Carino, N. J. (2001). “The Impact-Echo Method: An Overview.” Structures Congress & Exposition 2001, Washington, D.C.: American Society of Civil Engineers.

Carino, N.J. and Sansalone, M. (1990). “Flaw Detection in Concrete Using the Impact-Echo Method.” Proceedings, NATO Conference on Bridge Evaluation, Repair and Rehabilitation, A.S. Nowak, Ed., Kluwer Academic Publishers, Dordrecht, Netherlands, pp. 101-118.

Cheng, C. and Sansalone, M. (1993a). “The Impact-Echo Response of Concrete Plates Containing Delaminations: Numerical, Experimental, and Field Studies.” Materials and Structures, Vol. 26, No. 159, June, pp. 274-285.

Golden Software, LLC (2020). “User’s Guide: Contouring and 3D Surface Mapping for Scientists and Engineers.” Colorado, USA.

Gucunski, N., Imani, A., Romero, F., Nazarian, S., Yuan, D., Wiggenhauser, H., Shokouhi P., Taffe, A. and Kutrubes, D. 2012. “Nondestructive testing to identify concrete bridge deck deterioration.” The National Academies Press, Washington, DC, https://doi.org/10.17226/22771.

Impact-Echo User's Manual: A Self-Teaching Course and Reference for the Impact-Echo Method and Software Version 2.2a October 2001.

Kee, S.H., Gucunski, N. (2016). "Interpretation of Flexural Vibration Modes from Impact-Echo Testing." J. Infrastruct. Syst., 22(3): 04016009.

Lin, J. M., and Sansalone, M. (1997). "A Procedure for Determining P-wave Speed in Concrete for Use in Impact-Echo Testing Using a Rayleigh Wave Speed Measurement Technique." Innovations in Nondestructive Testing, SP-168, S. Pessiki and L. Olson, Eds., American Concrete Institute, Farmington Hills, MI, pp.137-165.

Mindlin, R., Schacknow, A. and Deresiewicz, H. (1956). "Flexural Vibrations of Rectangular Plates." J. Appl. Mech. 430-443.

Mitchell, A.K., Hazell C.R. (1987) "A Simple Frequency Formula for Clamped Rectangular Plates." Journal of Sound and Vibration 118(2), 271–281.

Oh, T., Popovics, J. S., and Sim, S.H. (2013b). "Analysis of Vibration for Regions Above Rectangular Delamination Defects in Solids." J. Sound Vibr., 332(7), 1766–1776.

Olson Istruments, Inc. (2016). "NDE 360 Platform with WinIE Software Version 2.5." Colorado, USA.

Sansalone, M. and Carino, N. J. (1986). "Impact-Echo: A Method for Flaw Detection in Concrete Using Transient Stress Waves." NBSIR 86-3452 (National Bureau of Standards, Gaithersburg, Maryland).

Shokouhi, P 2006. "Comprehensive Evaluation of Concrete Bridge Decks Using Impact Echo." Rutgers, The State University of New Jersey, New Jersey.

Significant Bottom Delamination, Photograph, viewed 1 June 2020, <http://www.dot.state.oh.us/Divisions/Engineering/Structures/bridge%20operations%20and%20maintenance/PreventiveMaintenanceManual/BPMM/repairs/Photos/pic203.jpg>.

Biographical Information

Mantaka Mahjabin Momo is pursuing her Masters of Science in Civil Engineering with a concentration in structural engineering in The University of Texas at Arlington. She earned her Bachelor of Science in Civil Engineering from Bangladesh University of Engineering and Technology (BUET) on September 2017. The focus of her undergraduate thesis was a finite element investigation of hollow square steel column sections under lateral loading, using ANSYS. Before joining UTA, she briefly worked as a graduate research assistant at the University of Louisiana at Lafayette, where she worked with dngineered cementitious composites (ECC).